RESEARCH ARTICLE

Synthesis of Zinc Nanoparticles using *Portulaca oleracea* Plant Extract

Sazan M. Haidary*

Department of Food Technology, College of Agricultural Engineering Sciences, Salahaddin University, Erbil, Iraq

Received: 24th February, 2022; Revised: 06th April, 2022; Accepted: 20th May, 2022; Available Online: 25th June, 2022

ABSTRACT

Zinc oxide (ZnO) nanoparticles (NPs) were successfully synthesized using green synthesis techniques, which was the focus of this study by using *Portulaca oleracea* extract, a reducing, capping, and stabilizing agent alongside with zinc acetate dihydrate acts as a precursor. The functionalization of Zn nanoparticles is investigated through (UV-vis) spectroscopy, X-ray diffraction (XRD), Fourier transform infrared (FTIR) spectroscopy, field emission scanning electron microscopy (FE-SEM), transmission electron microscopy (TEM), thermal gravimetric-differential thermal analysis (TG-DTA), dynamic light scattering DLS and zeta potential, energy dispersive X-ray spectroscopy (EDX), and Brunauer-Emmett-Teller (BET) analysis. UV-Vis- analysis revealed that the indirect bandgap of the biosynthesized ZnO NPs is 3.54 eV. In addition, the XRD and EDX analysis found that the structure of the nanoparticles is Wurtzite hexagonal with an average crystalline size of 16.58 nm. Moreover, the FT-IR spectra revealed the functional groups and the presence of ZnO NPs. According to the FE-SEM study, the average diameter of the grains was 95.53 nm. TEM analysis showed that the shape of the biosynthesized ZnO NPs was quasi-spherical, and their diameter was around 21.13 nm. Furthermore, DLS analysis demonstrated that the particle size distribution of ZnO NPs ranged from 40–55 nm. This study has that the specific surface area to volume ratios of the biosynthesized ZnO NPs was equal to 5.8772 m^2/g.

Keywords: Capping agent, Green synthesis method, *Portulaca oleracea*, Reducing agent, Stabilizing agent, ZnO Nanoparticles.

International Journal of Drug Delivery Technology (2022); DOI: 10.25258/ijddt.12.2.4

How to cite this article: Haidary SM. Synthesis of Zinc Nanoparticles using *Portulaca oleracea* Plant Extract. International Journal of Drug Delivery Technology. 2022;12(2):481-489.

Source of support: Nil.

Conflict of interest: None

INTRODUCTION

Nanotechnology is the most energetic investigation in current condensed material science, including nanoparticles. Nanoparticles are materials that include structures, devices, spherical, tubes, amorphous, and systems with different properties and roles, a 3D structure, changing in the magnitude of their atoms from one of the dimensions in 1–100 nm scale range.[1,2]

The importance of nanotechnology has received remarkable attention in science and is extensively used in biomedical technology, engineering, and medical applications due to its high surface area. Therefore, nanomaterials have been applications in numerous fields, such as catalysis, biomedicines, pharmaceutics, healthcare, food technology, textile industry, optics, optoelectronic devices, solar energy, magnetic field, etc.[3]

Metal and metal oxide nanoparticles have excellent antioxidant properties. They significantly inhibit microbial growth at low concentrations, which are commonly used.to detect pathogenic microbes and diagnose cancer progression.[2]

However, metal oxide nanoparticles such as calcium, magnesium oxide nanoparticles as reducing agents, and silver nanoparticles were synthesized using a green synthesis approach and demonstrated excellent antioxidant and antibacterial properties, but were less cytotoxic,[4-7] and zinc nanoparticles, with unusually unique optical, electrical, and magnetic capabilities, as well as a direct wide bandgap (3.3 eV) and considerable excitation binding energy (60 meV), have recently attracted a lot of attention because of their properties.[8,9]

Generally, ZnO nanoparticles can be synthesized through many different physicochemical methodologies, i.e., sol-gel processes that give homogenous precipitation,[9] laser vaporization, hydrothermal and solvothermal methods,[10] chemical vapor decomposition, mechanochemical milling, and molecular, microemulsion, and ball milling.[11,12]

Commonly, these preparation methods have several limitations due to their being not environmentally friendly, high cost, large area required for equipment set up, and other use of toxic chemicals.[13] To overcome these limitations, various methods were implemented to produce (ZnO) nanoparticles using different sources: plants extracted, bacteria, and fungus, but green chemistry synthesis in comparison with other physical and chemical methods is much safer and

*Author for Correspondence: sazan.haidar@su.edu.krd

environmentally friendly. Rapid, and low-cost, procedures have been attracted that do not produce toxic products for human use, and synthesis on a large scale without using high pressure, temperature, and energy.[14,15]

A green nanoparticle synthesis is a tool of choice that can be easily prepared. Researchers have recently explored synthesizing (ZnO) NPs using plants, leaves, fruits, and vegetables through a green synthesis method. Plant extracts are important because of an enormous number of phytochemicals, i.e., flavonoids, glycosides, polyphenol, terpenoids, and enzymes, acting as reducing, capping, and stabilizing agents.[16]

Here, zinc oxide ZnO NPs were synthesized using aqueous fruit extracts of *Myristica fragrans* as a reducing agent, and have anti-microbial, antileishmanial, anti-diabetic, antioxidant, anti-larvicidal, and protein kinase inhibitory activity.[17]

The green synthesis of ZnO NPs from *Euphorbia petiolate* and *Petroselinum crispum* using leaf extract plant with zinc nitrate hexahydrate salt as a precursor is performed in another study.[18,19] The anti-microbial and antioxidant properties of ZnO NPs with zinc nitrate hexahydrate have been reported along with substantial anti-microbial properties with *Escherichia coli* and *Staphylococcus aureus* bacteria.[20-22]

Abel synthesized ZnO NPs from aqueous leaf extracts of coffee, which were discovered to have a cubic form structure and diameters of 300 nm.[23]

Rubus fairholmianus root was used by Naresh Kumar Rajendran to synthesize ZnO NPs. Further, he studies the biosynthesized ZnO nanoparticles for antibacterial activity.[24]

This effort belongs to the green synthesis of nanoparticles area, and its application as a catalyst, gas sensor, drug delivery, biosensing, molecular diagnostics, solar cells, cell labeling, imaging, and optoelectronics.[13,25-27]

This study used a green synthesis method to prepare zinc oxide (ZnO) nanoparticles (NPs) from *P. oleracea*, often known as purslane. *P. oleracea* is a prominent edible annual herb found in Europe, Africa, North America, Australia, and Asia and can grow up to 30 cm tall with tiny leaves of oval shape and dark green color.[27]

The name, from the Latin, means "milk." Since the plant contains milky juice, it grows in orchards, gardens, crop fields, and on roadsides. *P. oleracea* is termed as a "vegetable for long life" in Chinese medical culture because it has been used in folk medicine to treat a wide range of illnesses, such as constipation.[28] Because it has a wide range of pharmacological effects, it is used as a pharmacopoeia.[29,30] Its chemical composition contains high levels of proteins, carotenoids, polysaccharides, and sterols.[31] It is an essential source of omega-3 fatty acids.[32,33] It also contains a lot of vitamins A, C, and E, as well as some B-complex vitamins and minerals (Se Ca, Fe, Mn, P, and P).

In addition, some literature has investigated the phenolic profile, antioxidant activity, and determination of volatile compounds, amino acids, anti-microbial assays, tocopherols etc. of *P. oleracea*.[34,35]

In the present study, ZnO NPs were synthesized for the first time using local *P. oleracea*, a reducing, capping, and stabilizing agent (Figure 1). Our study's development can be showcased via a detailed analysis of several factors influencing the ZnO nanoparticles morphology.[36]

MATERIALS AND METHODS

Plant Collection and Experimental Procedures

The *P. oleracea* plant was picked in July 2021 in Erbil, Iraq's Kurdistan region. The leaves steam of the *P. oleracea* plant (Figure 1). Dirty ads are collected and washed using deionized water to eradicate them. The 25 g of fresh *P. oleracea* plant were washed thoroughly and cut into smaller parts, which

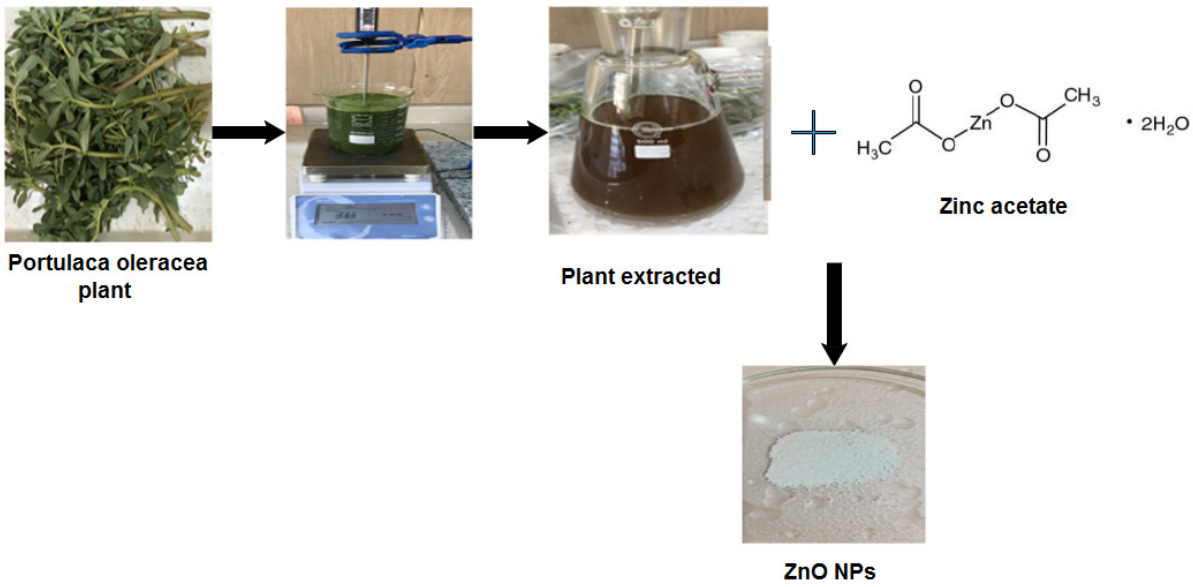

Figure 1: Flow chart for the synthesis of ZnO nanoparticles using portulaca oleracea plant extracts and zinc acetate

were placed in 250 milliliters of distilled water to form a paste, and then heated at 80°C for 40 minutes before being filtered and stored in a freezer for future use.

Materials used in the experiments were zinc acetate and Zn (CH3CO2).2H2O. Merck supplied the molecules [with a molecular weight of 297.48 g/mol and a purity greater than 98.0%]. To make the nanoparticles, 100 mL of plant extract from the *P. oleracea* plant was used. It was added to 100 mL of zinc acetate, which is zinc $(CH_3CO_2)2H_2O$.1 g of zinc acetate was dissolved in 50 mL of distilled water with magnetic stirring at 70°C for 30 minutes.

Then the color of the solution changed, and some snowy sedimentation occurred, which means that the reaction started and was separated by centrifugation at 8000 rpm at 60°C for 15 minutes. The solid powder was cleaned to remove the possible contamination and other organic materials with methanol and distilled water several times as a sign of the formation of ZnO NPs, and the residue was dried at 80°C for 2 hours in a hot air oven until dried.

Characterization of Zn Nanoparticles

The ZnO NPs structure morphology was characterized by UV-Vis spectroscopy double beam at a wavelength between 200 and 800 nm. FTIR spectrophotometer samples were recorded on a Perkin Elmer spectrophotometer with 200 potassium pressed into a pellet for FTIR characterization at the resolution of 4 cm^{-1} groups of prepared nanoparticles. This was used for the investigation of the functional group.

An XRD analysis was performed on an X-ray diffractometer using analytical X- Pert PRO (Cu Ka = 1.5406 A°). The scanning rate was 1°/ min in the θ–2θ range of 20 to 80°. X-ray crystallography determines the crystal density, purity, and size of the nanoparticles. Also, the shape and size were analyzed by FE-SEM (Quanta 4500). The chemical composition of the synthesized nanoparticle was characterized using an EDX.

Other than that, the morphological features of the particles were obtained through Transmission electron microscopy) (TEM; Philips CM120) using a Philips EM201C apparatus operating at 80 kV. Brunauer-Emmett-Teller (BET) surface area measurements were used to analyze the biosynthesized ZnO NPs surface area.

RESULT AND DISCUSSION

UV-vis Analysis

The optical features of phytochemicals present in the plant extract can reduce metal ions to metal nanoparticles. This was investigated by UV-vis spectroscopy and presented in Figure 2a. The absorption peak at 260 nm and 320 nm confirmed the phenolic compounds; tocopherol was the main vitamin E isoform. Because of available OH groups, this vitamin is considered the major phytochemical component of *P. oleracea* plant extract. For biosynthesized ZnO NPs, the absorption in the range of 250–270 nm is reported in the literature.[36]

Furthermore, the main sugars in the stems and leaves were glucose and fructose, which had omega-6 and omega-3 fatty acids, as well as more palmatic and linoleic acids than other sugars.[31]

The synthesis of ZnO NPs was also confirmed by (UV-vis) spectroscopy, as demonstrated in (Figure 2b). Additionally, an absorption peak was observed around 350 nm when the reaction between zinc acetate $(Zn(CH_3CO_2).2H_2O)$ and *P. oleracea* was extracted. The color of the mixture changed, which confirmed the formation of ZnO NPs. This is attributed to the electron transitions from the valence band to the conduction band. An indistinguishable result of the absorption band representing ZnO NPs was also obtained from other research with the absorption band range of 300 to 380 nm, similar to our study. In addition, the straightforward bandgap energy (Eg) for the ZnO NPs was calculated by fitting the reflection data to the straight transform Formula 1. E = the straight bandgap h = is blank constant, c = speed of light, λ = wavelength, which can be obtained from Figure 1. The wavelength of 350 nm corresponds to the indirect bandgap of the biosynthesized ZnO NPs is 3.54 eV.[37] Similar UV absorption was achieved at 366 nm by using polyol chemistry.[38]

$$E = hv = hc/\lambda \quad (1)$$

Scanning Electron Microscopy (SEM) and Transmission Electron Microscopy (TEM)

FESEM analysis was conducted to analyze the surface morphology of biosynthesized ZnO NPs (Figure 3a).

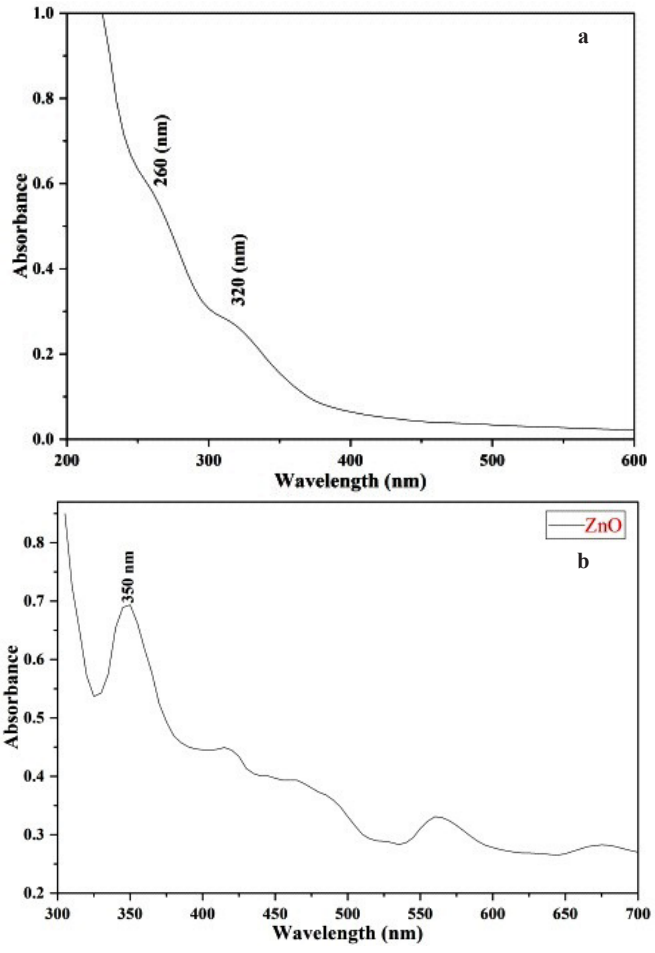

Figure 2: A- UV-vis spectrum of *P. oleracea* plant, **b-** UV-vis spectrum of ZnO NPs.

According to the FE-SEM investigation, hexagonal NPs with an average diameter of 95.53 nm was found in the fresh leaves aqueous extract of the plant biosynthesized ZnO NPs in different magnification ranges for instance, a range of 200 nm.[18,39] Besides, the ZnO NPs were prepared by precipitation and sol-gel procedures using zinc nitrate and zinc (II) acetylacetonate as ZnO precursors, with a size of 100 nm.[40]

The most significant amount of the ZnO NPs have the same dimension when seen collectively. Furthermore, broad findings confirmed somewhat agglomerated ZnO NPs, typical of green synthesis nanoparticles. This is since biosynthesis ZnO NPs possess a higher surface area, and the agglomeration may be caused by the polarity and electrostatic attraction of ZnO NPs.[17,39]

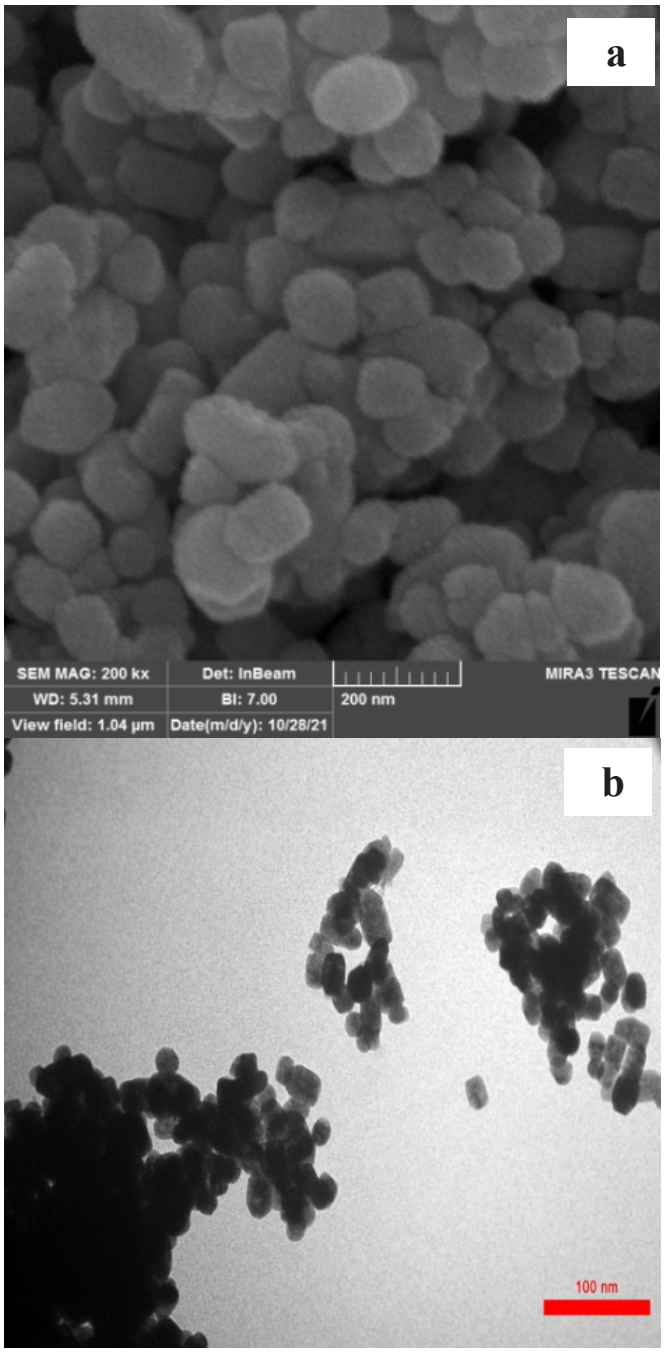

Figure 3.a: SEM image of biosynthesized ZnO NPs of prepared using zinc acetate as the Starting material. **3.B:** TEM images of prepared ZnO NPs

Figure 3(b) shows transmission electron microscopy (TEM) images of biosynthesized ZnO NPs from the extracted plant. It is made up of agglomerated Nano-scaled particles that are quasi-spherical in shape. According to TEM analysis, the shape of the biosynthesized ZnO NPs was quasi-spherical, with a diameter of roughly 21.13 nm; our findings were consistent with prior publications.[41,42] Furthermore, the size was 25 nm, as reported in the chemical synthesis of ZnO NPs by hydrothermal method.[43]

DLS and Zeta Potential

Dynamic light scattering investigations of biosynthesized ZnO NPs helped obtain the size distribution image of the particles (Figure 4a). The size distribution of ZnO NPs was between 40 and 55 nm. The average particle size distribution is 50 nm, which is more significant than SEM observations. The zeta potential of the biosynthesized ZnO NPs defines the colloidal stability and is a typical measurement of the surface charge on a particle in suspension, macromolecule, or material surface.[44]

The results of this study indicated a sharp peak at -39.5 mV (Figure 4b). The nanoparticles' surface is negatively charged and dispersed into the medium showing their stable and repulsive nature.[45]

EDX Analysis

The sample spectrum is confirmed via the EDX (Energy dispersive X-ray spectroscopy) analysis. Figure 5 shows the EDX spectrum of prepared nanoparticles. The element composition of the samples was determined using the EDX. The data was made up of three elements: Zn (51.29 %), O (26.41%), and C (26.41%), (22.30%). The presence of carbon in the suggested amount is due to the plant phytochemical group engaged in reducing and capping the biosynthesized ZnO NPs.[46,47] The weight percentages of Zn and O are close to the ZnO NPs prepared via a simple sol-gel method.[48]

XRD Analysis

X-ray pattern of biosynthesized ZnO NPs from aqueous plant extracted is shown in (Figure. 6) revealed the 2θ characteristic peaks of NPs at 31.85°, 34.51°, 36.35°, 47.67°, 56.75°, 63.03°, 66.42°, 68.10°, 69.28°, 72.69° and 77.19° for (100), (002), (101), (102), (110), (103), (200), (112), (201), (004) and (202) planes (Table 1) (Figure 5).

The peaks agreed with the given standard XRD (JCPDS Card) and suggest the possibility of hexagonal Wurtzite form of ZnO NPs. The peak showed in a narrow and robust direction. This indicates the optimum crystalline structure of ZnO NPs (Figure 6).

The average crystalline structure (D) was calculated according to Debye-Scherrer's formula using Debye–Scherrer's equation, $D = k./. \cos \theta$. Where 0.89 refers to Scherrer's constant, is λ a wavelength of X-rays equal to 0.15406 nm, θ refers to the direction angle, and is full width at high maximum [FWHM]

of diffraction Peak in Table 1, and the crystalline size of biosynthesized ZnO NPs was determined to be 16.50 nm.

Related results have been reported for flower extracts of Nyctanthes arbor-tristis with a crystalline size of 16.58.[49]

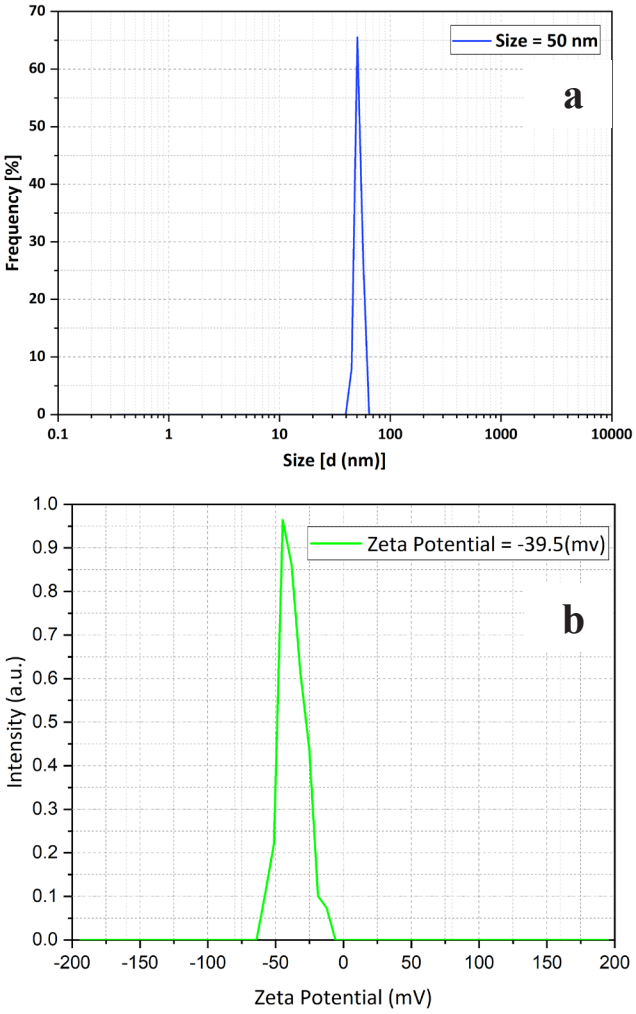

Figure 4: a- DLS size distribution potential and, **b**- ζ-potential distribution of *P. oleracea* plant extracted synthesized nanoparticles.

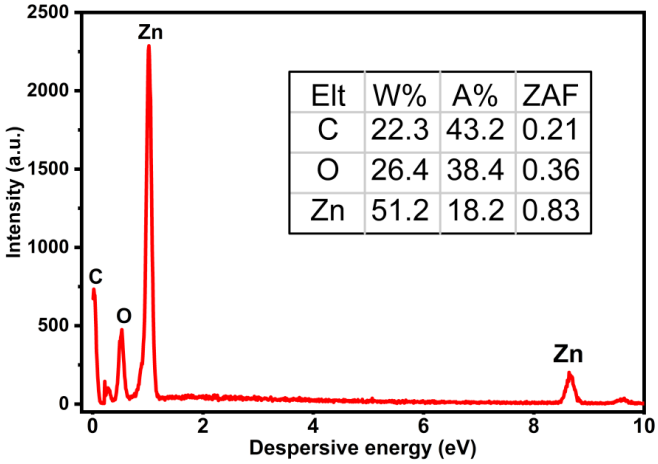

Figure 5: EDX spectrums of biosynthesized ZnO NPs using the extract of portulaca oleracea

Besides, the size was larger than 16.50 nm, and smaller than the 5.3689 reported in the chemical synthesis of ZnO NPs. The results confirmed that the ZnO NPs are of the wurtzite hexagonal type structure.[50,51]

Thermal stability

A thermo gravimetric analysis (TGA) has been conducted on the biosynthesized ZnO NPs. The decomposition behavior of green synthesized ZnO NPs was shown in Figure 7, throughout the temperature range of 100 to 600°C in an N_2 atmosphere. The first degradation process, which resulted in a 0.74% weight loss, began at 150°C and finished around 300°C, and was caused by evaporation of surface-adsorbed water. The second thermal degradation process, which began at 400 ° with weight loss 2.20 and ended around 500°C, could have been caused by the degradation of the condensation dehydration of the hydroxyls. Similar weight loss was also reported in other

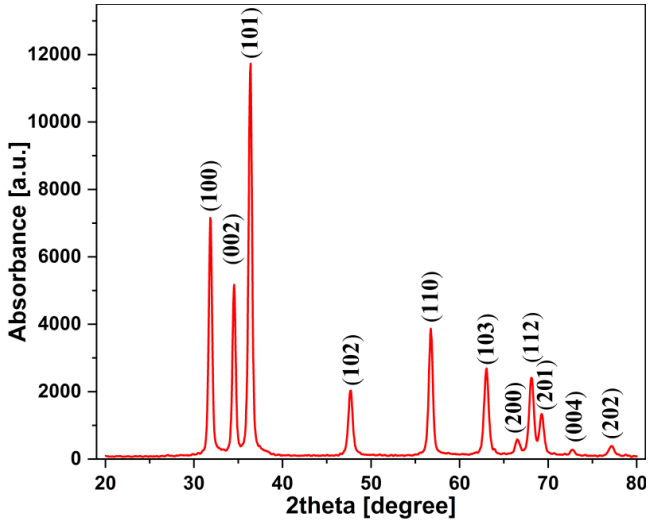

Figure 6: X-ray diffract gram of ZnO NPs

Table 1: The X-ray diffraction parameters and crystallite size of ZnO NPs using zinc acetate dihydrate with aqueous portulaca oleracea plant extracts

Average D (nm)	*D (nm)*	*FWHM*	*Peak position 20 (dgree)*
16.50	10.582702	0.7872	10.2546
	14.128691	0.5904	11.8032
	14.156576	0.5904	13.8159
	14.614714	0.5904	31.8505
	14.716129	0.5904	34.5102
	14.791916	0.5904	36.3528
	18.437576	0.492	47.678
	19.168215	0.492	56.7588
	16.485544	0.5904	63.0323
	20.157659	0.492	66.4274
	16.962817	0.5904	68.1087
	20.498297	0.492	69.2819
	20.938311	0.492	72.6943
	15.413517	0.6888	77.1983

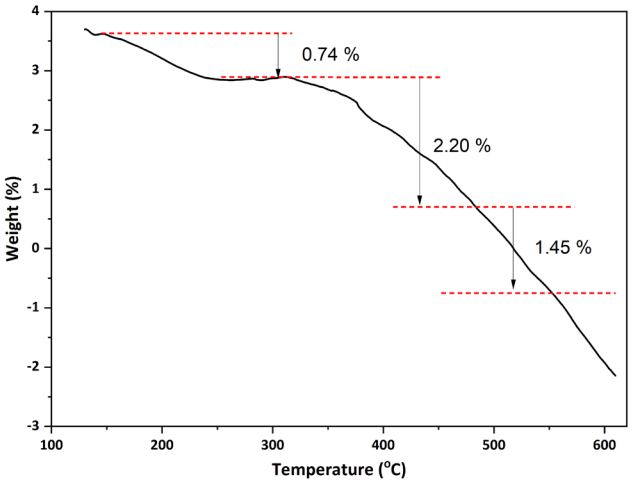

Figure 7: Thermo gravimetric analyses (TGA) of the biosynthesized ZnO NPs

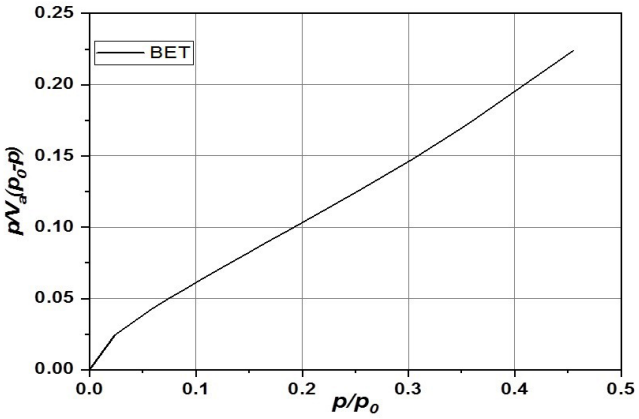

Figure 8: BET surface area analysis: Adsorption-desorption isotherms of ZnO NPs

research.[41,51-53] In addition, the degradation weight obtained from TGA agrees well with the curves of ZnO NPs synthesized using a mechanochemical method.[54]

Brunauer-Emmett-Teller (BET)

BET analysis of pore volume and average diameter (BJH) provides the evaluation of a precise specific surface conducted with high purity nitrogen at 77 K. as a function of relative pressure using a fully automated analyzer.[5]

The total specific surface area yielded valuable knowledge to explore the effects of surface porosity and particle size. The BET equation (2) was used to find the surface area of biosynthesized ZnO NPs. (Figure 8) illustrates nitrogen (N2) adsorption-desorption isotherms of ZnO NPs, as well as a typical type IV adsorption obtained from biosynthesized NPs, as classified by the IUPAC.[55] The isotherm relative was observed to have small adsorbent interaction potentials and was also associated with pores in the 1.5–100 nm range. The ZnO NPs powder has a specific surface area of S of 5.8772 m^2/g, which correlates to hexagonal particle size. A similar finding was discovered earlier.[56] While BET analysis revealed a surface area, pore volume and pore diameter of 9.259 m^2/g, and 9.87

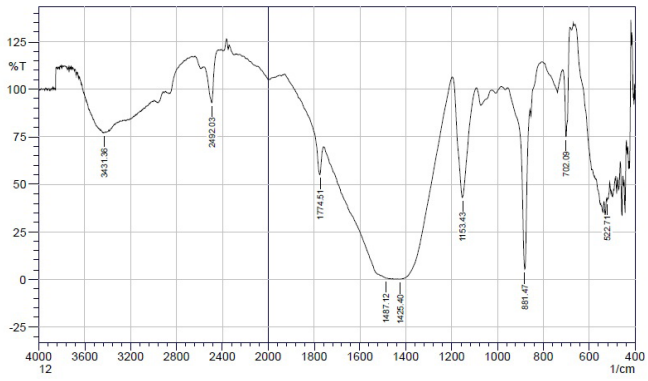

Figure 9: FT-IR spectrum of biosynthesized ZnO NPs

nm, respectively, they were prepared via a facile one-pot chemical precipitation approach.[51]

$$\frac{1}{W\left(\left(\frac{P_0}{P}\right)-1\right)} = \frac{1}{W_m C} + \frac{C-1}{W_m C}\left(\frac{P}{P_0}\right) \quad (2)$$

W= weight of gas adsorbed
P/P0 =relative pressure
Wm = weight of adsorbate as monolayer
C = BET constant

FTIR Spectroscopy Analysis

The typical FTIR spectrum is shown in Figure 9. This was performed to investigate and determine the functional group involved in biosynthesized ZnO NPs, which showed a peak in the (400–4000 cm^{-1}) spectral range. The samples have a typical FTIR spectrum for pure ZnO NPs, with absorption at 533 cm^{-1}, the characteristic absorption of the Zn-O bond, and broad absorption. The broadband at 3431.36 cm^{-1}, on the other hand, can be attributable to the phenolic compound's typical absorption of hydroxyl. This data is consistent with what others have found (Figure 9).[57-59]

These findings indicate that the Portulaca oleracea extract contains flavonoids, polyphenolics, and derivatives. Any shift or change in position or intensity was correlated to a functional group interaction with ZnO NPs. The appearance of new Peaks at 702.09 and 2492.03 cm^{-1} demonstrated that ZnO NPs had underwent.

The peaks at 1425.40 and 1487.12 cm^{-1} corresponded to the C–O and C–H bending and the carboxylic acid group stretching by 2492 cm^{-1}. At 1153 cm^{-1}, the bending vibration of the alcoholic –C–OH, –C=O groups from the aromatic ring with conjugation and the secondary alcoholic group was reflected. The FTIR analysis indicates that the prepared extract and ZnO NPs were rich in phenol and flavonoid components.[60,61]

CONCLUSIONS

ZnO NPs were positively synthesized from a green method using *P. oleracea* extract for the first time through a simple, cost-effective, and eco-friendly approach. Furthermore, this study indicated that the extract of *P. oleracea* has a potential impact. It helps as an effective reducing, capping, and stabilizing agent for the biological synthesis of ZnO NPs. The

biosynthesized ZnO NPs were characterized using techniques such as (UV-vis) spectroscopy, FTIR, SEM, TEM, EDX, XRD, DLS, TGA and BET analysis.

TGA analysis showed that the biosynthesized ZnO NPs possess thermal stability up to 500°C. The XRD analysis determines the crystallinity of the biosynthesized ZnO NPs, and presents all direction peaks fit well with the standard hexagonal Wurtzite structure. Moreover, XRD analysis showed that the average crystalline size of ZnO NPs was about 16.58 nm. TEM analysis showed that the biosynthesized nanoparticles' morphology was predominantly hexagonal. Finally, EDX analysis ensures the purity of ZnO NPs, and the optical band-gap energy is determined from UV-vis, was 3.54 eV.

ACKNOWLEDGEMENTS:

Primarily, the author would like to thank Salahaddin University in Erbil, Iraq. Furthermore, the authors express their gratitude to Dr. Azeez Abdullah Barzinjy and Mr. Kazem Qasem of Salahaddin University's College of Education's Nanotechnology Lab for providing all of the necessary facilities for conducting the research. In addition, the author thanks Dr. Ammar Z. Alshemary at Karabuk University. Finally, sincere thanks go to Kurd central research facilities in Erbil, Kurdistan region, Iraq.

REFERENCES

1. Hussain I, Singh N, Singh A, Singh H, Singh S. Green synthesis of nanoparticles and its potential application. *Biotechnology letters.* 2016;38(4):545-560.
2. Zhang D, Ma X-l, Gu Y, Huang H, Zhang G-w. Green synthesis of metallic nanoparticles and their potential applications to treat cancer. *Frontiers in Chemistry.* 2020:799.
3. Khan I, Saeed K, Khan I. Nanoparticles: Properties, applications and toxicities. *Arabian journal of chemistry.* 2019;12(7):908-931.
4. Khan H, Sakharkar M, Nayak A, Kishore U, Khan A. Nanoparticles for biomedical applications: An overview. *Nanobiomaterials.* 2018:357-384.
5. Kołodziejczak-Radzimska A, Jesionowski T. Zinc oxide—from synthesis to application: a review. *Materials.* 2014;7(4):2833-2881.
6. Rudramurthy GR, Swamy MK, Sinniah UR, Ghasemzadeh A. Nanoparticles: alternatives against drug-resistant pathogenic microbes. *Molecules.* 2016;21(7):836.
7. Vinardell MP, Llanas H, Marics L, Mitjans M. In vitro comparative skin irritation induced by nano and non-nano zinc oxide. *Nanomaterials.* 2017;7(3):56.
8. Alhadhrami A, Almalki A, Adam AMA, Refat MS. Preparation of semiconductor zinc oxide nanoparticles as a photocatalyst to get rid of organic dyes existing factories in exchange for reuse in suitable purpose. *Int J Electrochem Sci.* 2018;13(7):6503-6521.
9. Rouhi J, Mahmud S, Naderi N, Ooi CR, Mahmood MR. Physical properties of fish gelatin-based bio-nanocomposite films incorporated with ZnO nanorods. *Nanoscale research letters.* 2013;8(1):1-6.
10. Wang ZL. Zinc oxide nanostructures: growth, properties and applications. *Journal of physics: condensed matter.* 2004;16(25):R829.
11. Yue H, Fei W, Li Z, Wang L. Sol–gel process of ZnO and ZnAl2O4 coated aluminum borate whiskers. *Journal of sol-gel science and technology.* 2007;44(3):259-262.
12. Zak AK, Razali R, Abd Majid WH, Darroudi M. Synthesis and characterization of a narrow size distribution of zinc oxide nanoparticles. *International journal of nanomedicine.* 2011;6:1399.
13. Kolekar T, Bandgar S, Shirguppikar S, Ganachari V. Synthesis and characterization of ZnO nanoparticles for efficient gas sensors. *Arch Appl Sci Res.* 2013;5(6):20-28.
14. Kalpana V, Devi Rajeswari V. A review on green synthesis, biomedical applications, and toxicity studies of ZnO NPs. *Bioinorganic chemistry and applications.* 2018;2018.
15. Murali M, Mahendra C, Rajashekar N, Sudarshana M, Raveesha K, Amruthesh K. Antibacterial and antioxidant properties of biosynthesized zinc oxide nanoparticles from Ceropegia candelabrum L.–an endemic species. *Spectrochimica Acta Part A: Molecular and Biomolecular Spectroscopy.* 2017;179:104-109.
16. Sharma D, Sabela MI, Kanchi S, et al. Biosynthesis of ZnO nanoparticles using Jacaranda mimosifolia flowers extract: synergistic antibacterial activity and molecular simulated facet specific adsorption studies. *Journal of Photochemistry and Photobiology B: Biology.* 2016;162:199-207.
17. Ovais M, Khalil AT, Islam NU, et al. Role of plant phytochemicals and microbial enzymes in biosynthesis of metallic nanoparticles. *Applied microbiology and biotechnology.* 2018;102(16):6799-6814.
18. Faisal S, Jan H, Shah SA, et al. Green synthesis of zinc oxide (ZnO) nanoparticles using aqueous fruit extracts of Myristica fragrans: their characterizations and biological and environmental applications. *ACS omega.* 2021;6(14):9709-9722.
19. A Barzinjy A. Characterization of ZnO Nanoparticles Prepared from Green Synthesis Using Euphorbia Petiolata Leaves. *Eurasian Journal of Science & Engineering.* 2019;4(3):74-83.
20. Barzinjy AA, Azeez HH. Green synthesis and characterization of zinc oxide nanoparticles using Eucalyptus globulus Labill. leaf extract and zinc nitrate hexahydrate salt. *SN Applied Sciences.* 2020;2(5):1-14.
21. Ambika S, Sundrarajan M. Antibacterial behaviour of Vitex negundo extract assisted ZnO nanoparticles against pathogenic bacteria. *Journal of Photochemistry and Photobiology B: Biology.* 2015;146:52-57.
22. Dobrucka R, Długaszewska J. Biosynthesis and antibacterial activity of ZnO nanoparticles using Trifolium pratense flower extract. *Saudi journal of biological sciences.* 2016;23(4):517-523.
23. Kalpana V, Payel C, Rajeswari VD. Lagenaria siceraria aided green synthesis of ZnO NPs: anti-dandruff, Anti-microbial and Anti-arthritic activity. *Research Journal of Chemistry and Environment.* 2017;21(11):14-19.
24. Abel S, Tesfaye JL, Shanmugam R, et al. Green Synthesis and Characterizations of Zinc Oxide (ZnO) Nanoparticles Using Aqueous Leaf Extracts of Coffee (Coffea arabica) and Its Application in Environmental Toxicity Reduction. *Journal of Nanomaterials.* 2021;2021:3413350.
25. Rajendran NK, George BP, Houreld NN, Abrahamse H. Synthesis of zinc oxide nanoparticles using Rubus fairholmianus root extract and their activity against pathogenic bacteria. *Molecules.* 2021;26(10):3029.
26. Qu J, Luo C, Hou J. Synthesis of ZnO nanoparticles from Zn-hyperaccumulator (Sedum alfredii Hance) plants. *Micro & Nano Letters.* 2011;6(3):174-176.
27. Thema F, Manikandan E, Dhlamini M, Maaza M. Green synthesis of ZnO nanoparticles via Agathosma betulina natural extract. *Materials Letters.* 2015;161:124-127.

28. Uddin M, Juraimi AS, Hossain MS, et al. Purslane weed (Portulaca oleracea): a prospective plant source of nutrition, omega-3 fatty acid, and antioxidant attributes. *The Scientific World Journal.* 2014;2014.
29. Xu X, Yu L, Chen G. Determination of flavonoids in Portulaca oleracea L. by capillary electrophoresis with electrochemical detection. *Journal of Pharmaceutical and Biomedical Analysis.* 2006;41(2):493-499.
30. Chan K, Islam M, Kamil Ma, et al. The analgesic and anti-inflammatory effects of Portulaca oleracea L. subsp. sativa (Haw.) Celak. *Journal of ethnopharmacology.* 2000;73(3):445-451.
31. Zidan Y, Bouderbala S, Djellouli F, Lacaille-Dubois M, Bouchenak M. Portulaca oleracea reduces triglyceridemia, cholesterolemia, and improves lecithin: cholesterol acyltransferase activity in rats fed enriched-cholesterol diet. *Phytomedicine.* 2014;21(12):1504-1508.
32. Petropoulos SA, Fernandes Â, Dias MI, et al. Nutritional value, chemical composition and cytotoxic properties of common purslane (Portulaca oleracea L.) in relation to harvesting stage and plant part. *Antioxidants.* 2019;8(8):293.
33. Voynikov Y, Gevrenova R, Balabanova V, Doytchinova I, Nedialkov P, Zheleva-Dimitrova D. LC-MS analysis of phenolic compounds and oleraceins in aerial parts of Portulaca oleracea L. *Journal of Applied Botany and Food Quality.* 2019;92:298-312.
34. Alam M, Juraimi AS, Rafii M, et al. Evaluation of antioxidant compounds, antioxidant activities, and mineral composition of 13 collected purslane (Portulaca oleracea L.) accessions. *BioMed research international.* 2014;2014.
35. Farag MA, Shakour ZTA. Metabolomics driven analysis of 11 Portulaca leaf taxa as analysed via UPLC-ESI-MS/MS and chemometrics. *Phytochemistry.* 2019;161:117-129.
36. Fernández-Poyatos MdP, Llorent-Martínez EJ, Ruiz-Medina A. Phytochemical composition and antioxidant activity of Portulaca oleracea: Influence of the steaming cooking process. *Foods.* 2021;10(1):94.
37. Erkan N. Antioxidant activity and phenolic compounds of fractions from Portulaca oleracea L. *Food Chemistry.* 2012;133(3):775-781.
38. Ezealisiji KM, Siwe-Noundou X, Maduelosi B, Nwachukwu N, Krause RWM. Green synthesis of zinc oxide nanoparticles using Solanum torvum (L) leaf extract and evaluation of the toxicological profile of the ZnO nanoparticles–hydrogel composite in Wistar albino rats. *International Nano Letters.* 2019;9(2):99-107.
39. Mahamuni PP, Patil PM, Dhanavade MJ, et al. Synthesis and characterization of zinc oxide nanoparticles by using polyol chemistry for their antimicrobial and antibiofilm activity. 2019;17:71-80.
40. Ramesh M, Anbuvannan M, Viruthagiri G. Green synthesis of ZnO nanoparticles using Solanum nigrum leaf extract and their antibacterial activity. *Spectrochimica Acta Part A: Molecular and Biomolecular Spectroscopy.* 2015;136:864-870.
41. Uribe-López M, Hidalgo-López M, López-González R, et al. Photocatalytic activity of ZnO nanoparticles and the role of the synthesis method on their physical and chemical properties. 2021;404:112866.
42. Zheng Y, Fu L, Han F, et al. Green biosynthesis and characterization of zinc oxide nanoparticles using Corymbia citriodora leaf extract and their photocatalytic activity. *Green Chemistry Letters and Reviews.* 2015;8(2):59-63.
43. Duraimurugan J, Kumar GS, Maadeswaran P, Shanavas S, Anbarasan P, Vasudevan V. Structural, optical and photocatlytic properties of zinc oxide nanoparticles obtained by simple plant extract mediated synthesis. *Journal of Materials Science: Materials in Electronics.* 2019;30(2):1927-1935.
44. Madathil ANP, Vanaja K, Jayaraj M. Synthesis of ZnO nanoparticles by hydrothermal method. Paper presented at: Nanophotonic materials IV2007.
45. Modena MM, Rühle B, Burg TP, Wuttke S. Nanoparticle Characterization: Nanoparticle Characterization: What to Measure?(Adv. Mater. 32/2019). *Advanced Materials.* 2019;31(32):1970226.
46. Bala N, Saha S, Chakraborty M, et al. Green synthesis of zinc oxide nanoparticles using Hibiscus subdariffa leaf extract: effect of temperature on synthesis, anti-bacterial activity and anti-diabetic activity. *RSC Advances.* 2015;5(7):4993-5003.
47. Rezaei A, Abdollahi H, Derikvand Z, Hemmati-Sarapardeh A, Mosavi A, Nabipour N. Insights into the effects of pore size distribution on the flowing behavior of carbonate rocks: Linking a nano-based enhanced oil recovery method to rock typing. *Nanomaterials.* 2020;10(5):972.
48. Santhoshkumar J, Kumar SV, Rajeshkumar S. Synthesis of zinc oxide nanoparticles using plant leaf extract against urinary tract infection pathogen. *Resource-Efficient Technologies.* 2017;3(4):459-465.
49. Hedayati K. Fabrication and optical characterization of zinc oxide nanoparticles prepared via a simple sol-gel method. 2015.
50. Jamdagni P, Khatri P, Rana J. Green synthesis of zinc oxide nanoparticles using flower extract of Nyctanthes arbor-tristis and their antifungal activity. *Journal of King Saud University-Science.* 2018;30(2):168-175.
51. Oladiran AA, Olabisi IA-MJIJoAP. Synthesis and characterization of ZnO nanoparticles with zinc chloride as zinc source. 2013;2(2).
52. Akpomie KG, Ghosh S, Gryzenhout M, Conradie JJSr. One-pot synthesis of zinc oxide nanoparticles via chemical precipitation for bromophenol blue adsorption and the antifungal activity against filamentous fungi. 2021;11(1):1-17.
53. El-Arab NB. Synthesis and characterization of zinc oxide nanoparticles using green and chemical synthesis techniques for phenol decontamination. *Int J Nanoelectron Mater.* 2018;11(2):179-194.
54. Fatimah I, Pradita RY, Nurfalinda A. Plant extract mediated of ZnO nanoparticles by using ethanol extract of Mimosa pudica leaves and coffee powder. *Procedia engineering.* 2016;148:43-48.
55. Moballegh A, Shahverdi H, Aghababazadeh R, Mirhabibi AJSS. ZnO nanoparticles obtained by mechanochemical technique and the optical properties. 2007;601(13):2850-2854.
56. Bahri S, Omdurman S. KINETIC AND THERMODYNAMIC STUDIES OF TRIVALENT ARSENIC REMOVAL BY INDIUM-DOPED ZINC OXIDE NANOPOWDER.
57. Ismail M, Taha K, Modwi A, Khezami L. ZnO nanoparticles: Surface and X-ray profile analysis. *J Ovonic Res.* 2018;14:381-393.
58. Demissie MG, Sabir FK, Edossa GD, Gonfa BA. Synthesis of zinc oxide nanoparticles using leaf extract of lippia adoensis (koseret) and evaluation of its antibacterial activity. *Journal of chemistry.* 2020;2020.
59. Girma M. *Synthesis Of Zinc Oxide Nanoparticle Using Leaf Extract Of Lippia Adoensis (Koseret) And Evaluation Of Its Antibacterial Activity*, ASTU; 2018.

60. Yedurkar S, Maurya C, Mahanwar P. Biosynthesis of zinc oxide nanoparticles using ixora coccinea leaf extract—a green approach. *Open Journal of Synthesis Theory and Applications.* 2016;5(1):1-14.

61. Alamdari S, Sasani Ghamsari M, Lee C, et al. Preparation and characterization of zinc oxide nanoparticles using leaf extract of Sambucus ebulus. *Applied Sciences.* 2020;10(10):3620.